

**Spatial modeling of Audubon Christmas Bird Counts reveals fine-scale patterns and
drivers of relative-abundance trends**

TIMOTHY D. MEEHAN^{1†}, NICOLE L. MICHEL², AND HÅVARD RUE³

¹ *National Audubon Society, Boulder, Colorado, USA*

² *National Audubon Society, Portland, Oregon, USA*

³ *King Abdulla University of Science and Technology, Thuwal, Saudi Arabia*

† **E-mail:** tmeehan@audubon.org

12

Abstract. Bird counts by community volunteers provide valuable information about the conservation needs of many bird species. The statistical modeling techniques commonly used to analyze these counts provide robust, long-term population trend estimates from heterogeneous community science data at regional, national, and continental scales. Here we present a new modeling approach that increases the spatial resolution of trend estimates and reduces the computational burden of trend estimation, each by an order of magnitude. We demonstrate the approach with data for the American Robin (*Turdus migratorius*) from Audubon Christmas Bird Counts conducted between 1966 and 2017. We show that aggregate regional trend estimates from the proposed method aligned well with those from the current standard method, and that spatial variation in trends were associated with winter temperatures and human population densities as predicted by ecological energetics. This technique can provide reasonable large-scale trend estimates for users interested in general patterns, while also providing higher-resolution estimates for examining correlates of abundance trends at finer spatial scales, which is a prerequisite for tailoring management plans to local conditions.

Key words: Audubon Christmas Bird Count, Bayesian hierarchical model, conditional autoregressive model, North American Breeding Bird Survey, population trends, range shifts, spatially varying coefficients model

INTRODUCTION

Volunteers with the Audubon Christmas Bird Count (CBC) have been counting wintering birds across North America every year for the last 118 years (Dunn et al. 2005, Soykan et al. 2016). Population trends derived from CBC data, along with those derived from other large-

scale monitoring programs like the North American Breeding Bird Survey (BBS, Robbins et al. 1989, Sauer et al. 2017), provide valuable information for understanding the conservation needs of North American bird species (Dickinson et al. 2010, Hochachka et al. 2012). For example, CBC and BBS trends are used to evaluate population change rates and population half-lives for many of the 448 bird species included in the Partners in Flight Landbird Conservation Plan (Rosenberg et al. 2016, 2017). CBC and BBS trends are also used by BirdLife International (<http://datazone.birdlife.org/species/search>) to make status recommendations to the International Union for Conservation of Nature, creators of the Red List of Threatened Species (<https://www.iucnredlist.org/>), and by the North American Bird Conservation Initiative (NABCI) to produce their State of the Birds conservation vulnerability assessment for all 1,154 native North American bird species (NABCI 2016). CBC trends are especially useful for species who are otherwise not monitored in their remote northern breeding locations, particularly those that breed in the poorly-surveyed boreal forest or Arctic tundra (Niven et al. 2004, Roy et al. *in review*).

The current, standard approach for generating trends from CBC data (Link et al. 2006, Soykan et al. 2016) was derived from methods originally developed for BBS data (Link and Sauer 2002, Sauer and Link 2011). The general approach is to assign counts in Canada and the US to one of up to 169 spatial strata, which are intersections of US states or Canadian provinces, and Bird Conservation Regions (BCR, Sauer et al. 2003). Then, treating each stratum as independent, a non-linear function is used to correct for the effect of observer effort on counts, while simultaneous effects are estimated for the impact of count circle, year, and stratum by year (Link et al. 2006, Soykan et al. 2016). These parameter estimates are used to derive a relative abundance index per stratum and year, and those annual indices are used to compute annual

percent change per stratum across defined time periods (Link and Sauer 2002, Sauer and Link
60 2011).

The standard CBC analysis provides robust long-term trend estimates from
62 heterogeneous community science data across large spatial scales. By pooling count circles per
stratum, this approach deals with the issue of count circles haphazardly becoming active or
64 inactive over the time series (Sauer and Link 2011, Soykan et al. 2016). Additionally, pooling
produces a sufficiently large sample of counts to generate a reasonably robust count-effort
66 correction function (Link and Sauer 1999), which is critical given the wide variation in count
effort among count circles (Bock and Root 1981, Dunn et al. 2005). This approach produces a
68 relative abundance index per year and stratum, which can be used to explore variation around
long-term log-linear trends, and can be summed across larger hierarchically-nested strata, such as
70 states, provinces, BCRs, or Landscape Conservation Cooperative (LCC) regions, and used to
estimate change in relative abundance at larger spatial scales. Producing annual abundance
72 indices also permits summarizing abundance change between any desired pair of time points.
Finally, the simplicity of the standard model enables a flexible and robust computational process,
74 suitable for analysis of hundreds of species that vary enormously in their ubiquity, abundance,
and population dynamics.

76 While the current approach produces trends that are useful for understanding population
status of birds at regional to continental scales, the approach has some limitations. As
78 implemented, it is a computationally intensive process, especially for wide-ranging species. This
is due to the use of Markov chain Monte Carlo (MCMC) to estimate model parameters for
80 relative abundance, and processing large MCMC chains to scale relative abundance to larger
aggregate units to generate change estimates.

82 From an ecological perspective, the coarse resolution of standard population trend
analyses limits their ability to provide inference about local variation, processes, and drivers.
84 While trends can be scaled up to larger spatial units, they cannot be scaled down to smaller ones.
The analytical stratum is the finest level of resolution, which limits the extent to which variation
86 in trends can be attributed to fine-scale processes such as change in local land cover or weather
patterns (Thogmartin et al. 2004, Bled et al. 2013), and limits opportunities for tailoring
88 conservation plans to local conditions (Ethier and Nudds 2015, Ethier et al. 2017). Abundance,
distribution, and population trends of birds are affected by land cover, climate, topography, and
90 other environmental conditions and processes at a variety of spatial scales ranging from local
(e.g., home range or smaller) to landscape (Thogmartin et al. 2004, 2006; Zhang et al. 2012).
92 Summarizing and evaluating correlates of trends at the scale of traditional strata may miss
important regional variation in abundance, distribution, and the environmental conditions
94 affecting them.

 Moreover, the current approach does not take full account or advantage of spatial
96 relationships among counts. Modeling this structure would facilitate borrowing information
across spatial boundaries, allowing more robust trend estimates in places where data are sparse
98 (Waller and Gotway 2004, Banerjee et al. 2014, Blangiardo and Cameletti 2015) and enabling
trend estimation at finer spatial scales (Thogmartin et al. 2004, Bled et al. 2013). Accounting for
100 the spatial dependence across count sites also reduces the amount of spatial autocorrelation in
model residuals, which leads to more reliable inference about trend estimates (Dormann et al.
102 2007, Beale et al. 2010).

 Previous work by Thogmartin et al. (2004), Bled et al. (2013), and Smith et al. (2015),
104 among others, offered spatially-explicit variations of the standard trend analysis approach for

community science data. These works were focused on analysis of BBS data, but their
106 approaches are easily applied to analysis of CBC data. Instead of using the standard strata
described above (Smith et al. 2015), Thogmartin et al. (2004) assigned count sites to irregular
108 polygons, created by tessellation of BBS route locations. Bled et al. (2013) assigned routes to
cells on a regular grid, with one-degree latitude and longitude spacing. All three studies utilized
110 spatially-structured random intercepts for relative abundance per polygon, grid cell, or stratum.
Thogmartin et al. (2004) included an effect of year per polygon, but that effect did not
112 incorporate spatial structure. Bled et al. (2013) and Smith et al. (2015) estimated relative
abundances per year, and then trends were generated as derived parameters, as done in the
114 standard analysis.

Here, we present a new approach for calculating temporal trends in relative abundance,
116 one that takes advantage of the considerable spatial structure in CBC data. This approach
borrows components from previous ones, incorporates new components that prioritize robust
118 trend estimation at finer spatial scales, and employs a simplified and computationally efficient
workflow. Similar to Bled et al. (2013), we assigned CBC count sites to cells on a uniform grid
120 that covered North America. In contrast to previous work, effort and year effects were modeled
as random slopes with spatial structure, following a spatially-varying coefficient (SVC) approach
122 (Gelfand et al. 2003, Finley 2011, Congdon 2014). Finally, unlike prior studies using MCMC,
we used integrated nested Laplace approximation (INLA) to estimate Bayesian posteriors for
124 model parameters (Rue et al. 2009, Martins et al. 2013, Lindgren and Rue 2015, Blangiardo and
Cameletti 2015, Rue et al. 2017, Bakka et al. 2018, Krainski et al. 2018), which led to a dramatic
126 decrease in computing time. Our objective in developing this technique was to estimate long-
term population trends at an appropriate spatial scale for evaluating fine-scale population

processes and ecological drivers to inform conservation. The four goals of this report were to (i) describe an SVC approach for calculating trends in CBC data, (ii) employ the approach using data for the American Robin, (iii) compare trend results derived from the SVC approach to aggregate results derived from standard methods, and (iv) demonstrate use of fine-scaled trend results through a simple analysis exploring correlations between SVC trends and potential energetic drivers related to climate and winter food resources.

MATERIALS AND METHODS

Christmas Bird Count

We demonstrate use of the SVC approach using data from the CBC, a volunteer bird monitoring program begun in 1900. Since its inception, the program has grown tremendously, and now includes more than 2,400 count sites and involves more than 70,000 volunteers (Soykan et al. 2016). The program extends across North and South America, but the majority of counts have been conducted in the US and Canada. The program has produced counts extending 118 years, but standard trend analyses are conducted using counts conducted after 1965, as protocols and count efforts have been most consistent since then. An individual CBC occurs over a 24-hour period, once per year, during late December or early January. During a count, volunteers record birds seen or heard within a circular study area with a 24.1 km diameter. The area covered and the amount of time spent counting birds in a given circle varies considerably across years and count locations, so annual effort metrics are recorded and used to standardize bird counts. More details about the CBC can be found in Bock and Root (1981) and Dunn et al. (2005), who describe the program and discuss the potential uses and limitations of CBC data.

Statistical model

We modeled CBC count data, $y_{i,k,t}$, for grid cell i encompassing count circle k during year t , as a random variable from a negative binomial distribution. Expected values for counts per grid cell, $\mu_{i,t}$, were assumed to be a function of spatially-structured grid-cell, count-effort, and year effects, plus unstructured variation among count circles. The linear predictor for $\mu_{i,t}$ took the form:

$$\log(\mu_{i,t}) = \alpha_i + \epsilon_i \log(E_{i,k,t}) + \tau_i T_{i,k,t} + \kappa_k. \quad (\text{Eq. 1})$$

Parameters α_i were modelled as cell-specific random intercepts with an intrinsic conditional autoregressive (CAR) structure (Besag et al. 1991). With this structure, α_i values came from a normal distribution, with a conditional mean related to the average of adjacent cells, and with conditional variance proportional to the variance across adjacent cells and inversely proportional to the number of adjacent cells. Spatial structure was incorporated into α_i to allow for information about relative abundance to be shared across neighboring cells, and to reduce the spatial autocorrelation among model residuals that occurs when this spatial structure is ignored (Dormann et al. 2007, Finley 2011).

Parameters ϵ_i were modeled as spatially-structured, cell-specific, random slope coefficients for the effort effect. These spatially-varying coefficients (Gelfand et al. 2003, Banerjee et al. 2014, Congdon 2014) were also modelled with a CAR structure (Besag et al. 1991). Slopes were drawn from a normal distribution with a conditional mean related to the average of adjacent cells, and with conditional variance proportional to the variance across adjacent cells and inversely proportional to the number of adjacent cells. Spatial structure was

incorporated into ϵ_i to allow for information about the effort effect to be shared across neighboring cells, and to accommodate a potential lack of stationarity in the effort effect (Finley 2011). Effort was represented by $E_{i,j,k}$, the number of party hours expended during a count, where a party hour was the count effort of one party of unspecified size for one hour. Pairing log-transformed counts with log-transformed effort in the linear predictor yielded a power function for effort correction, a flexible mathematical form that accommodated a decreasing, linear, or increasing impact of effort on expected counts (Butcher and McCulloch 1990, Link and Sauer 1999).

Parameters τ_i were modeled as spatially-structured, cell-specific, random slope coefficients for the year effect. Spatially-varying τ_i coefficients (Gelfand et al. 2003, Banerjee et al. 2014, Congdon 2014) were also modeled with CAR structure (Besag et al. 1991), where values came from a normal distribution, with conditional means and variances as described above. Spatial structure was incorporated into τ_i to allow for information about the year effect to be shared across neighboring cells, and to allow the year effect to vary across the cells in the study region. Year, represented by T , was transformed before analysis such that $\max(T) = 0$, and each preceding year took an increasingly-negative integer value. Given the scaling of effort and year variables, $\exp(\alpha_i)$ could be interpreted as a cell-specific expected count given one party hour of effort during the final year in the time series.

The final term in the model, κ_k , was an exchangeable random effect that accounted for variation in relative abundance among circles, possibly due to differences in habitat conditions or observer experience (Soykan et al. 2016). Note that the model did not include a normally-distributed, observation-level random effect to deal with overdispersed Poisson counts, i.e., $y | \epsilon \sim \text{Poisson}(\mu\epsilon)$ and $\epsilon \sim \text{Normal}(\mu, \sigma)$, as is done for the standard approach (Sauer and Link

2011, Soykan et al. 2016). Rather, we used a negative binomial count distribution for y , i.e.,
198 $y | \varepsilon \sim \text{Poisson}(\mu\varepsilon)$ and $\varepsilon \sim \text{Gamma}(\phi^{-1}, \phi^{-1})$ (Linden and Mantyniemi 2011). These two
approaches are expected to yield similar outcomes. However, as implemented in R-INLA, the
200 latter approach returns a single dispersion estimate while foregoing estimation of individual
observation effects, which reduces computing time and the size of posterior samples.

202 *Case study data*

204 We developed a case study, using data for the American Robin (*Turdus migratorius*)
from CBCs conducted across the continental US and Canada between 1966 and 2017, to
206 demonstrate the SVC modeling approach, compare results with those from the standard
approach, and illustrate a straightforward analysis of fine-scaled trends. Before modeling the
208 CBC data, extreme outliers (> 3 SD from the mean, after log transformation) in counts and effort
were removed. After filtering, there were 36,650,191 American Robins encountered in 78,140
210 counts from 3,195 count circles over 52 years, available for modeling.

Locations of the 3,195 unique count circles were mapped using the North American
212 Albers Equal Area Conic projection (EPSG 102008, <https://epsg.io/102008>) and assigned to 880
cells on a grid divided along 100 km increments in latitude and longitude (Fig. 1A). Grid cells
214 formed a continuous lattice within a non-convex polygon created using circle locations. The
number of count circles per grid cell varied from 0 to 20, and averaged 2.43 (Fig. 1A). The
216 number of neighbors for a given grid cell ranged from 1 to 8, and averaged 7.48. Note that grid
cells with zero counts were retained during model estimation to preserve the spatial relationships
218 between counts. However, before analyzing resulting trend estimates, cells with no observed

counts were removed from the dataset, as we were not interested in interpolating trends for grid
cells without CBC sites.

Model computation

The SVC model described above was analyzed within a Bayesian framework using the R-INLA package (version 18.10.09, Martins et al. 2013, Lindgren and Rue 2015, Blangiardo and Cameletti 2015, Rue et al. 2017, Bakka et al. 2018, Krainski et al. 2018) for R statistical computing software (version 3.3.1, R Core Team 2016). For parameters α_i , ϵ_i , and τ_i , with CAR structure, precision matrices were scaled such that the geometric mean of marginal variances was equal to one (Sørbye and Rue 2014, Riebler et al. 2016, Freni-Sterrantino et al. 2018), and priors for precision parameters were penalized complexity (PC) priors, with parameter values $U_{pc} = 1$ and $a_{pc} = 0.01$ (Simpson et al. 2017). Precision for the zero-centered, exchangeable, random circle effect, κ_k , was also assigned a PC prior with parameter values $U_{pc} = 1$ and $a_{pc} = 0.01$ (Simpson et al. 2017). The overdispersion term for the negative binomial count distribution, ϕ , was assigned a PC prior with parameter value $l = 7$. Very simply, as implemented here, PC priors were weakly informative priors with an innate tendency to shrink structured and unstructured random effects toward zero in the absence of a strong signal. Readers are referred to Simpson et al. (2017) for the details of, and rationale behind, PC priors, as well as the default structures and parameter values of PC priors used in the R-INLA package.

Along with parameter estimates, R-INLA produced values to evaluate individual model fit (Czado et al. 2009) and compare different models to one another (Gneiting and Raftery 2007, Link et al. 2017): cross-validation probability integral transform (PIT, Dawid 1984) and conditional predictive ordinate (CPO, Pettit 1990). For this application, we were not comparing

multiple models. However, we extracted PIT values and visually inspected their histogram, as an approximate uniform distribution is expected for a model that fits the data reasonable well (Czado et al. 2009, Held et al. 2010).

Following model analysis, posterior medians and symmetric 95% credible intervals were computed per cell for α_i , ϵ_i , and τ_i . Credible interval widths, representing estimate uncertainty, were computed by subtracting the lower credible limit from the upper credible limit per cell. Posterior summaries were then mapped to visualize spatial variation in abundance indices, effort effects, and relative-abundance trends.

Trend comparisons

It is common, following CBC and BBS analyses, to aggregate trend information to larger scales that might be of interest to resource managers designing and implementing policies across states, provinces, BCRs, LCCs, or nations (Sauer et al. 2003, Sauer and Link 2011, Soykan et al. 2016). After analysis of the SVC model for the American Robin, we aggregated 100 km results to the BCR level in order to compare them to those produced using standard CBC analysis methods (Soykan et al. 2016). SVC trends were aggregated for each BCR by averaging trends for all equal-area grid cells where the cell centroid fell within the BCR. We evaluated the uncertainty around SVC trend estimates by comparing credible interval widths for cells within a BCR to those calculated for a BCR using the standard approach. We note that full posterior distributions for aggregate SVC trend estimates could have been computed by averaging random draws from τ_i posteriors for cells within a BCR, or by using R-INLA functions for creating linear combinations (Blangiardo and Cameletti 2015). Further, those averages could have been weighted by the amount of area where the cells and BCR overlap (Bled et al. 2013). We did not

employ these methods here because our main focus was on fine scale trends and only qualitative
266 comparison with standard results.

268 *Correlates of American Robin trends*

One of the greatest potential benefits of the SVC method is the ability to produce fine-
270 scale population trends, enabling investigation of both fine- and coarse-scale ecological
processes and population trend drivers. To highlight this potential, we conducted a simple
272 demonstration analysis of fine-scaled American Robin trends. Specifically, we explored
correlations between SVC abundance trends and three covariates: latitude, historic minimum
274 winter temperature, and historic human population density.

We expected that, in the Northern Hemisphere, latitude would be positively related to
276 SVC trends, as several landbird species have demonstrably shifted their ranges towards the
Earth's poles (Thomas and Lennon 1999, La Sorte and Thompson 2007, Huang et al. 2017). A
278 northward range shift would logically lead to negative trends in the southern portion of their
range and positive trends in the northern portion of their range. One putative mechanism for
280 northward range shifts in wintering birds is the increase in minimum winter temperatures across
the continent over the past 50 years (Zuckerberg et al. 2011, Princé and Zuckerberg 2015), which
282 makes the energetics of wintering in the north more favorable (Root 1988, Meehan et al. 2004).
With this mechanism in mind, we expected that, for a given latitude, residual trends would be
284 negatively related to historic minimum winter temperature, as birds began wintering in
historically colder locations further from coasts and higher in elevation. Finally, we tested the
286 hypothesis that winter bird distribution and abundance is also governed by resource availability
(Dunning and Brown 1982, Meehan et al. 2004). We expected that, after accounting for latitude

and minimum winter temperature, SVC trends would be positively related to historic human population density (Robb et al. 2008, Zuckerberg et al. 2011), as American Robins are well known to prosper in human-dominated landscapes, replete with mown grass and fruiting ornamentals (Beissinger and Osborne 1982, Marzluff 1997).

For this analysis, τ_i values were related to the latitude of the centroid for a given 100 km grid cell. A single, historical-average minimum December and January temperature was calculated per cell between 1965 and 2017, using the CRU TS v4.01 dataset (Harris et al. 2014). A single, historic-average human population size between 1970 and 2015 was calculated per cell using Global Population Count Grid Time Series Estimates (CIESIN 2017) for 1970 and the GPWv4 dataset (CIESIN 2016) for 2015. Cell specific τ_i values were modeled with a latent Gaussian model, where $\tau_i \sim \text{Normal}(\mu_i, \sigma^2)$, $\mu_i = \beta_0 + \beta_1 L_i + \beta_2 T_i + \beta_3 (P_i^{0.25}) + v_i$, and L_i , T_i , and P_i represented cell-specific latitude, historic-average minimum winter temperature, and historic-average human population size variables, respectively. Note the transformation of P_i , which was highly right-skewed. The term v_i represented cell-specific random intercepts with CAR structure (Besag et al. 1991), where the precision matrix was scaled such that the geometric mean of marginal variances was equal to one (Sørbye and Rue 2014, Riebler et al. 2016, Freni-Sterrantino et al. 2018). v_i was added to the model to account for spatial structure in the model residuals (Dormann et al. 2007, Beale et al. 2010). $\beta_0, \beta_1, \beta_2$, and β_3 were given normal priors with mean of zero and precision equal to 0.001. The prior for precision associated with the CAR term was a PC prior (Simpson et al. 2017) with parameter values $U_{pc} = 0.1$ and $a_{pc} = 0.01$.

RESULTS

On average, 4.28 robins were counted per party hour in 2017, but that number varied by several orders of magnitude across the species range, from 0.01 to 73.50. A map of posterior median values illustrated that the species was most abundant in the central part of their range, and was least abundant along the northern and southern margins of their range (Fig. 1B). Analysis of the SVC model using R-INLA took approximately 10 minutes to complete. Inspection of the PIT histogram indicated satisfactory model fit.

Posterior median values for ϵ_i , the power-law exponent for the relationship between effort and counts, varied from 0.28 to 1.44, with a median value of 0.81. The 95% credible intervals for ϵ_i values indicated that 80% of estimates were not significantly different from 1, while all were significantly greater than 0. Estimates not significantly different from 1 indicated a positive linear relationship between effort and counts. Values significantly greater than 0 and less than 1 also indicated a positive relationship between effort and counts, but one with diminishing returns for additional count effort. A map of posterior median ϵ_i values highlighted the spatial structure in the effort effect (Fig. 1C). Locations with posterior medians well below 1 were frequently locations with relatively low abundance indices (Fig. 1B), suggesting that the majority of American Robins in a count circle could be counted with relatively low effort. Locations with posterior medians closer to 1 were frequently locations with relatively high abundance indices (Fig. 1B), suggesting an endless supply of American Robins for CBC volunteers to count. The two parameters, α_i and ϵ_i , were correlated across space, with a rank correlation coefficient of 0.26.

Posterior median values for τ_i , the temporal trend from 1966 through 2017, when transformed to annual percent change, varied from -11.80% to 13.63%, with a median value of 2.63% (Fig. 1D). The 95% credible intervals for τ_i values indicated that 8% of estimates were

significantly lower than 0, while 44% were significantly greater than 0 (Fig. 1E). A map of
 334 posterior median τ_i values showed that relative abundance trends had strong spatial structure.
 Credible intervals for τ_i values (Fig. 1F) were used to illustrate where trends were significantly
 336 negative or positive, showing that relative abundance during winter has generally decreased in
 the southern and coastal parts of their range and increased in the northern and interior parts of
 338 their range. The parameters α_i and τ_i were significantly correlated across space, with a rank
 correlation coefficient of -0.16, indicating that the strongest trends were occurring at the margins
 340 of the geographic range where relative abundance was lowest.

The posterior median estimate for ϕ , the dispersion parameter, was $\exp[-\log(0.55)] =$
 342 1.83, considerably larger than 1, highlighting overdispersion in American Robin counts relative
 to a Poisson distribution. Credible intervals for precision estimates for the random effects
 344 showed that all were important for explaining variation in the count data. When precision values
 were converted to a standard deviation scale, the random effects were ranked α_i (SD = 1.58), κ_k
 346 (1.05), ϵ_i (0.25), and τ_i (0.04), in terms of the amount of variation explained.

Figure 2 shows the median of posterior median SVC trends across cells per BCR (Fig.
 348 2A), along with the posterior median trend for each BCR from the standard analysis (Fig. 2B).
 Side-by-side visual comparison of these maps showed that aggregate trends were similar,
 350 regardless of method. The SVC approach gave a median trend of 2.11% across all BCRs, while
 the posterior median trend for the standard approach was 1.95% across all BCRs. Within BCRs,
 352 the trend direction was consistent across the two methods in 28 of 32 BCRs. The rank
 correlation between BCR trends generated by the two methods was 0.88. Regarding differences,
 354 trends derived from the SVC approach changed more smoothly across the continent, as would be
 expected using a spatial statistical model. Also, the range of posterior median SVC trends (-

4.58% to 9.16%) was slightly less than that for standard trends (-7.96% to 14.26%), especially near geographic range boundaries, as would be expected given the sharing of information across space.

Figure 3 compares the credible interval widths for SVC trends per grid cell (Fig. 3A) with those from the standard approach for aggregate BCR estimates (Fig. 3B). When compared to the standard approach, some SVC grid cells within a BCR, ones in information rich neighborhoods (Fig.1A), had SVC trend estimates with remarkably narrow confidence intervals (Fig. 3C, SVC minimum). Other grid cells, ones in information poor neighborhoods (Fig.1A), had trend estimates with relatively broad confidence intervals (Fig. 3C, SVC maximum). On average, however, precision of estimates per BCR were similar, regardless of method, if not slightly higher using the SVC approach (Fig. 3C, SVC median).

As predicted, trends were positively related to degrees north latitude, with trends being negative at low latitudes and positive at high latitudes (Fig. 4A), suggesting a poleward shift in winter range for the American Robin. After accounting for latitude, there was a clear negative relationship between historic average minimum temperature and SVC trends (Fig. 4B), indicating that robins were becoming more abundant in historically colder areas at higher elevations and further from coasts. After accounting for latitude and historic minimum winter temperature, SVC trends were positively related to the number of people historically residing in a grid cell, which we use as a proxy for resource availability for this anthropophilic species.

DISCUSSION

This analysis demonstrated use of Bayesian SVC models to estimate fine-scaled, long-term relative abundance trends along with their environmental drivers from community science

data collected across North America. The inclusion of spatially-structured random slope terms
380 allowed for robust estimation of effort effects and relative abundance trends at spatial resolutions
much finer than the standard analysis approach. The use of INLA for model analysis resulted in
382 dramatically reduced computing time compared to the standard analysis approach. Fine scaled
trend estimates for the American Robin, when aggregated to the BCR level, were very similar to
384 those produced by the standard analysis approach. When we explored correlates of American
Robin SVC trends, we found that trends were related to latitude, historic winter temperature, and
386 historic human population size as expected from the literature on factors governing the
distribution and abundance of wintering birds.

388 To put resolution gains into context, consider that a CBC circle has a radius of
approximately 12 km and an area of 452 km². A 100 km grid cell, covering 10,000 km², is
390 approximate 22 times larger than a CBC circle. In comparison, the average analytical stratum
has an area of 104,378 km², approximately 231 times the area of a CBC circle. Thus, the SVC
392 approach brought an order of magnitude increase in spatial resolution when compared to the
standard approach. This increased resolution facilitated finer-scaled investigations into the
394 drivers of winter bird trends (Thogmartin et al. 2004, Bled et al. 2013, Smith et al. 2015).
Understanding the fine-scale drivers of trends creates opportunities to tailor conservation plans to
396 local conditions (Ethier and Nudds 2015, Ethier et al. 2017).

Estimating trends at relatively high resolution was made possible by adopting spatial-
398 statistical techniques designed to borrow information across neighboring regions (Thogmartin et
al. 2004, Bled et al. 2013, Smith et al. 2015). Employing spatial techniques also had
400 implications for uncertainty in trend estimates. In the standard analysis, the uncertainty in a trend
estimate depended upon the variation in trends across the circles within a stratum and the number

of circles in a stratum. In the SVC analysis, uncertainty depended upon those same two factors, but also depended upon those characteristics in the neighborhood of a grid cell. The consequences of this difference are demonstrated in Figure 3. In regions with many CBC circles (e.g., Piedmont BCR), SVC methods produced trend estimates with relatively low uncertainty (minimum credible interval width of 1.48%) compared to the standard method (3.40%), due to the density of information. Similar to Bled et al. (2013), we found that precision of SVC estimates also tended to be relatively high in regions at the edge of a species range where there were few counts (e.g., Boreal Softwood Shield BCR, maximum interval width of 12.02%) when compared to the standard approach (19.14%), due to borrowing of information across neighboring cells that crossed regional boundaries. In other parts of the continent with fewer, more isolated CBC circles (e.g., Southern Rockies Colorado Plateau BCR), the SVC methods produced trend estimates with relatively high uncertainty (minimum interval width of 3.47%) compared to the standard method (2.80%). It is not entirely clear if the small intervals of the standard approach are justified in this context. If the relatively few and far-between circles that fall within those large BCRs can be considered representative samples of that larger area, then estimates with high precision are reasonable, and certainly preferred. If it cannot be assumed that those circles are representative of the larger area, then estimating trends for smaller areas, in neighborhoods with more information, and basing uncertainty estimates on the amount of local information, seems more appropriate. Critical evaluation of this representative-sample assumption is particularly important when analyzing data from the CBC, because count-site selection is not based on sampling design principles, and count locations tend to be biased toward areas of high human population density and areas of high bird density and diversity (Drennan 1981, Dunn et al. 2005).

On a typical laptop computer, SVC model analysis using R-INLA took roughly 10
426 minutes for full Bayesian results. The standard approach, which employs MCMC, took
approximately 10 hours for full Bayesian results on the same hardware. Had spatial statistical
428 models been analyzed using MCMC, processing times would have been much longer. The
difference in computing time was due to R-INLA producing highly accurate approximations of
430 Bayesian posteriors, orders of magnitude faster than MCMC (Rue et al. 2009, 2017). The
obvious benefit of shorter processing times is that, for a given set of computing resources, more
432 time periods, more distinct model forms (e.g., Link and Sauer 2016), or more species can be
evaluated. Even small differences in computing time add up when analyzing counts from tens of
434 years, for hundreds of species, across thousands of count sites.

There were, as there usually are, tradeoffs for rapid model analysis. Specifically, R-
436 INLA is an analysis option whenever a statistical model can be expressed as a latent Gaussian
model (Rue et al 2009, Blangiardo and Cameletti 2013, Rue et al. 2017). This was possible for
438 the model used in this analysis. However, this would not have been possible had we chosen to
use the effort-correction function developed by Link and Sauer (1999, 2006) and used in the
440 standard analysis (Soykan et al. 2016). Here, we used a single-parameter, power-law function
for effort correction because it could fit positive, negative, linear, increasing, and decreasing
442 relationships (Butcher and McCulloch 1990) and was easily incorporated into a latent Gaussian
model. In contrast, the effort-correction function used for the standard approach is a two-
444 parameter nonlinear function, which is more flexible and so will better-fit relationships that come
to a rapid asymptote. Ideally, we would have tools for rapid analysis of spatial statistical models
446 that incorporate the standard effort-correction function. In this choose-two situation, we erred
towards rapid analysis of a spatial model with the simpler effort-correction function, because it

448 allowed for more robust, if occasionally slightly biased (Link and Sauer 1999), estimates of the
effort effect in regions where information was sparse. Robust estimates of effort effects are
450 particularly critical when generating trends from CBC data, as count effort varies widely across
time and space (Bock and Root 1981, Butcher et al. 1990, Dunn et al. 2005).

452 We note that the SVC approach described here differed from the standard approach in
that it was optimized, specifically, for computing long-term, log-linear trends in relative
454 abundance at fine spatial scales. The emphasis on long-term, log-linear trends was motivated by
requests from resource managers, who desire simple summary statistics that reflect overall
456 population status for many species (Rosenberg et al. 2016, 2017). The emphasis on fine spatial
resolution was motivated by requests from, both, researchers wishing to conduct research at
458 relatively fine spatial scales, and Audubon Christmas Bird Count volunteers, who wish to learn
how bird numbers have changed over the years in their local area. Given these two emphases, we
460 did not incorporate additional model terms necessary for creating annual abundance indices.
These indices are critical for those who wish to look beyond single, long-term trends, at detailed
462 time series that give more information about the nature of abundance changes (Sauer and Link
2002, 2011). Creating these annual indices is done by adding an additional random effect per
464 cell and year, and combining these effects with α and τ . Adding this effect to the SVC model is
easily done in R-INLA. This effect could be specified as exchangeable, or have spatial or
466 temporal structure. For this dataset, preliminary trials showed that adding an exchangeable
effect to the model increased computing time to approximately 1 hour. We did not explore this
468 model variant in depth because producing annual abundance indices was not a primary goal of
this effort.

When we applied the SVC approach to data from the American Robin, we learned that aggregate trends resulting from the SVC and standard approaches were similar in direction and magnitude. Precision at aggregate levels was generally similar, if not a bit lower with the SVC approach, due to different assumptions about how precision should, or should not, be related to the spatial distribution of counts. Spatial variation in SVC trends for the American Robin were also consistent with expectations from the literature on factors governing winter bird distribution and abundance (Root 1988, Meehan et al. 2004, La Sorte and Thompson 2007, Zuckerberg et al. 2011). Specifically, trends were negative at low latitudes, positive at high latitudes and, for a given latitude, were more positive in historically cold regions and in areas with higher human population density. While it is likely that latitudinal effects would have been found using aggregate trends from the standard analysis (Fig. 2), it is less likely that residual winter temperature and human population density effects would have been detected. This is because winter temperatures and human population sizes both tend to vary at spatial scales considerably finer than analytical strata, states, provinces or BCRs. Future studies could explore relationships between SVC trends and other potential variables that can be summarized at comparable spatial scales, such as forest management practices, agricultural intensification, and other factors related to land use and land cover.

Dunn et al. (2005) suggested that analyses of CBC data by the broader scientific community would increase in number and quality as preprocessed, effort-corrected trends were made available to the public, as they have been for the BBS results (Sauer et al. 2003). Work by Soykan et al. (2016) marks the initial outcome of an effort by Audubon to make this happen, and standard trend analysis results have recently become publically available via the internet for over 500 species (<https://www.audubon.org/conservation/where-have-all-birds-gone>). With further

fine tuning, it is possible that SVC trends could also become publically available for researchers
interested in conducting finer-scaled analyses of preprocessed, effort-corrected trends and their
environmental drivers.

ACKNOWLEDGEMENTS

We thank the thousands of volunteers who participate in the Audubon Christmas Bird
Count.

LITERATURE CITED

Bakka, H., H. Rue, G. A. Fuglstad, A. Riebler, D. Bolin, J. Illian, E. T. Krainski, D. P. Simpson,
and F. K. Lindgren. 2018. Spatial modeling with R-INLA: a review. *WIREs Computational
Statistics* e1443.

Banerjee, S., B. P. Carlin, and A. E. Gelfand. 2014. Hierarchical modeling and analysis for
spatial data. CRC Press, Boca Raton, Florida, USA.

Beale, C. M., J. J. Lennon, J. M. Yearsley, M. J. Brewer, and D. A. Elston. 2010. Regression
analysis of spatial data. *Ecology Letters* 13:246–264.

Beissinger, S. R., and D. R. Osborne. 1982. Effects of urbanization on avian community
organization. *Condor* 84:75–83.

Besag, J., J. York, and A. Mollié. 1991. Bayesian image restoration, with two applications in
 516 spatial statistics. *Annals of the Institute of Statistical Mathematics* 43:1–59.

518 Blangiardo, M., and M. Cameletti. 2015. *Spatial and spatio-temporal Bayesian models with R-INLA*. John Wiley and Sons, New York, New York, USA.

520

Bled, F., J. R. Sauer, K. Pardieck, P. Doherty, and J. A. Royle. 2013. Modeling trends from
 522 North American Breeding Bird Survey data: a spatially explicit approach. *PLoS ONE* 8:e81867.

524 Bock, C. E., and T. L. Root. 1981. The Christmas Bird Count and avian ecology. *Studies in Avian Biology* 6:17–23.

526

Butcher, G. S., M. R. Fuller, L. S. McAllister, and P. H. Geissler. 1990. An evaluation of the
 528 Christmas Bird Count for monitoring population trends of selected species. *Wildlife Society Bulletin* 18:129–134.

530

Butcher, G. S., and C. E. McCulloch. 1990. The influence of observer effort on the number of
 532 individual birds recorded on Christmas Bird Counts. Pages 120–129 *in* J. R. Sauer and S. Droege, editors. *Survey designs and statistical methods for the estimation of avian population trends*. Biological Report 90. US Fish and Wildlife Service, Washington, DC, USA.

534

536 Center for International Earth Science Information Network (CIESIN). 2016. Gridded population of the world, version 4, GPWv4, population count. <http://dx.doi.org/10.7927/H4BG2KXS>

538

Center for International Earth Science Information Network (CIESIN). 2017. Global population

540 count grid time series estimates, version 1, 1970-2000. <https://doi.org/10.7927/H4CC0XNV>

542 Congdon, P. 2014. Applied Bayesian modelling. John Wiley and Sons, New York, New York,
USA.

544

Czado, C., T. Gneiting, and L. Held. 2009. Predictive model assessment for count data.

546 Biometrics 65:1254–1261.

548 Dawid, A. P. 1984. Statistical theory: the prequential approach. Journal of the Royal Statistical
Society, Series A 147:278–292.

550

Dickinson, J. L., B. Zuckerberg, and D. N. Bonter. 2010. Citizen science as an ecological

552 research tool: challenges and benefits. Annual Review of Ecology, Evolution, and Systematics
41:149–172.

554

Dormann, C. F., J. M. McPherson, M. B. Araujo, R. Bivand, J. Bolliger, G. Carl, R. G. Davies,

556 A. Hirzel, W. Jetz, W. D. Kissling, I. Kuhn, R. Ohlemüller, P. R. Peres-Neto, B. Reineking, B.

Schröder, F. M. Schurr, R. Wilson. 2007. Methods to account for spatial autocorrelation in the

558 analysis of species distributional data: a review. Ecography 30:609–628.

560 Drennan, S. R. 1981. The Christmas Bird Count: an overlooked and underused sample. *Studies*
in *Avian Biology* 6:24–29.

562

Dunn, E. H., C. M. Francis, P. J. Blancher, S. R. Drennan, M. A. Howe, D. Lepage, C. S.

564 Robbins, K. V. Rosenberg, J. R. Sauer, and K. G. Smith. 2005. Enhancing the scientific value of
the Christmas Bird Count. *Auk* 122:338–346.

566

Dunning, J. B., and J. H. Brown. 1982. Summer rainfall and winter sparrow densities: a test of

568 the food limitation hypothesis. *Auk* 99:123–129.

570 Ethier, D. M., N. Koper, and T. D. Nudds. 2017. Spatiotemporal variation in mechanisms driving
regional-scale population dynamics of a threatened grassland bird. *Ecology and Evolution*

572 7:4152–4162.

574 Ethier, D. M., and T. D. Nudds. 2015. Scalar considerations in population trend estimates:
implications for recovery strategy planning for species of conservation concern. *Condor*

576 117:545–559.

578 Finley, A. O. 2011. Comparing spatially-varying coefficients models for analysis of ecological
data with non-stationary and anisotropic residual dependence. *Methods in Ecology and Evolution*

580 2:143–154.

582 Freni-Sterrantino, A., M. Ventrucchi, and H. Rue. 2018. A note on intrinsic conditional
 autoregressive models for disconnected graphs. *Spatial and Spatio-Temporal Epidemiology*
 584 26:25–34.

586 Gelfand, A. E., H. J. Kim, C. F. Sirmans, and S. Banerjee. 2003. Spatial modeling with spatially
 varying coefficient processes. *Journal of the American Statistical Association* 98:387–396.

588 Gneiting, T., and A. E. Raftery. 2007. Strictly proper scoring rules, prediction, and estimation.
 590 *Journal of the American Statistical Association* 102:359–378.

592 Harris, I., P. D. Jones, T. J. Osborn, and D. H. Lister. 2014. Updated high-resolution grids of
 monthly climatic observations: the CRU TS3.10 dataset. *International Journal of Climatology*
 594 34:623–642.

596 Held, L., B. Schrödle, and H. Rue. 2010. Posterior and cross-validators predictive checks: a
 comparison of MCMC and INLA. Pages 91-110 *in* T. Kneib and G. Tutz, editors. *Statistical*
 598 *modelling and regression structures*. Springer-Verlag, Berlin, Germany.

600 Hochachka, W. M., D. Fink, R. A. Hutchinson, D. Sheldon, Wong, Weng-Keen, and S. Kelling.
 2012. Data-intensive science applied to broad-scale citizen science. *Trends in Ecology and*
 602 *Evolution* 27:130–137.

604 Huang, Q., J.R. Sauer, and R.O. Dubayah. 2017. Multidirectional abundance shifts among North
 American birds and the relative influence of multifaceted climate factors. *Global Change*
 606 *Biology* 23:3610-3622.

608 Krainski, E. T., V. Gómez-Rubio, H. Bakka, A. Lenzi, D. Castro-Camilo, D. P. Simpson, F. K.
 Lindgren, and H. Rue. 2018. Advanced spatial modeling with stochastic partial differential
 610 equations using R and INLA. CRC Press, Boca Raton, Florida, USA.

612 La Sorte, F. A., and F. R. Thompson. 2007. Poleward shifts in winter ranges of North American
 birds. *Ecology* 88:1803–1812.

614

Linden, A., and S. Mantyniemi. 2011. Using the negative binomial distribution to model
 616 overdispersion in ecological count data. *Ecology* 92:1414–1421.

618 Lindgren, F., and H. Rue. 2015. Bayesian spatial modelling with R-INLA. *Journal of Statistical*
Software 63:19.

620

Link, W. A., and J. R. Sauer. 1999. Controlling for varying effort in count surveys: an analysis of
 622 Christmas Bird Count data. *Journal of Agricultural, Biological, and Environmental Statistics*
 4:116–125.

624

Link, W. A., and J. R. Sauer. 2002. A hierarchical analysis of population change with application
 626 to cerulean warblers. *Ecology* 83:2832–2840.

628 Link, W. A., and J. R. Sauer. 2016. Bayesian cross-validation for model evaluation and selection,
with application to the North American Breeding Bird Survey. *Ecology* 97:1746–1758.

630

Link, W. A., J. R. Sauer, and D. K. Niven. 2006. A hierarchical model for regional analysis of
632 population change using Christmas Bird Count data, with application to the American black
duck. *Condor* 108:13–24.

634

Link, W. A., J. R. Sauer, and D. K. Niven. 2017. Model selection for the North American
636 Breeding Bird Survey: a comparison of methods. *Condor* 119:546–556.

638 Martins, T. G., D. P. Simpson, F. K. Lindgren, and H. Rue. 2013. Bayesian computing with
INLA: new features. *Computational Statistics and Data Analysis* 67:68–83.

640

Marzluff, J. M. 1997. Effects of urbanization and recreation on songbirds. Pages 89-102 *in* W.
642 M. Block and D. M. Finch, editors. Songbird ecology in southwestern ponderosa pine forests: a
literature review. RMRS GTR-292. USDA Forest Service, Rocky Mountain Research Station,
644 Fort Collins, Colorado, USA.

646 Meehan, T. D., W. Jetz, and J. H. Brown. 2004. Energetic determinants of abundance in winter
landbird communities. *Ecology Letters* 7:532–537.

648

Niven, D. K., J. R. Sauer, G. S. Butcher, and W. A. Link. 2004. Christmas Bird Count provides
650 insights into population change in land birds that breed in the boreal forest. *American Birds*
58:10–20.

652

North American Bird Conservation Initiative (NABCI). 2016. The state of North America’s
654 birds, 2016. Environment and Climate Change Canada, Ottawa, Ontario, Canada.

656 Pettit, L. I. 1990. The conditional predictive ordinate for the normal distribution. *Journal of the*
Royal Statistical Society, Series B 52:175–184.

658

Princé, K., and B. Zuckerberg. 2015. Climate change in our backyards: the reshuffling of North
660 America’s winter bird communities. *Global Change Biology* 21:572–585.

662 Riebler, A., S. H. Sørbye, D. P. Simpson, and H. Rue. 2016. An intuitive Bayesian spatial model
for disease mapping that accounts for scaling. *Statistical Methods in Medical Research* 25:1145–
664 1165.

666 Robb, G. N., R. A. McDonald, D. E. Chamberlain, and S. Bearhop. 2008. Food for thought:
supplementary feeding as a driver of ecological change in avian populations. *Frontiers in*
668 *Ecology and the Environment* 6:476–484.

670 Robbins, C. S., J. R. Sauer, R. S. Greenberg, and S. Droege. 1989. Population declines in North
 American birds that migrate to the Neotropics. *Proceedings of the National Academy of Sciences*
 672 of the USA 86:7658–7662.

674 Root, T. 1988. Energy constraints on avian distributions and abundances. *Ecology* 69:330–339.

676 Rosenberg, K. V., P. J. Blancher, J. C. Stanton, and A. O. Panjabi. 2017. Use of North American
 Breeding Bird Survey data in avian conservation assessments. *Condor* 119:594–606.

678 Rosenberg, K. V., J. A. Kennedy, R. Dettmers, R. P. Ford, D. Reynolds, J. D. Alexander, C. J.
 680 Beardmore, P. J. Blancher, R. E. Bogart, and G. S. Butcher. 2016. Partners in Flight landbird
 conservation plan: 2016 revision for Canada and continental United States. Partners in Flight
 682 Science Committee.

684 Roy, C., N. L. Michel, C. Burkhalter, K. Gurney, C. Handel, D. Messmer, K. Prince, C. Rushing,
 J. Saracco, R. Schuster, A. Smith, P.A. Smith, P. Solymos, L. Venier, S. Van Wilgenburg, and B.
 686 Zuckerberg. *In review*. Monitoring boreal avian populations: how can we estimate trends and
 trajectories from noisy data?

688 Rue, H., S. Martino, and N. Chopin. 2009. Approximate Bayesian inference for latent Gaussian
 690 models by using integrated nested Laplace approximations. *Journal of the Royal Statistical*
 Society, Series B 71:319–392.

692

Rue, H., A. Riebler, S. H. Sørbye, J. B. Illian, D. P. Simpson, and F. K. Lindgren. 2017.

694 Bayesian computing with INLA: a review. *Annual Review of Statistics and its Application*
4:395–421.

696

Sauer, J. R., J. E. Fallon, and R. Johnson. 2003. Use of North American Breeding Bird Survey
698 data to estimate population change for bird conservation regions. *Journal of Wildlife*
Management 67:372–389.

700

Sauer, J. R., and W. A. Link. 2002. Using Christmas Bird Count data in analysis of population
702 change. *American Birds* 102:10–14.

704 Sauer, J. R., and W. A. Link. 2011. Analysis of the North American Breeding Bird Survey using
hierarchical models. *Auk* 128:87–98.

706

Sauer, J. R., K. L. Pardieck, D. J. Ziolkowski Jr, A. C. Smith, M.-A. R. Hudson, V. Rodriguez,
708 H. Berlanga, D. K. Niven, and W. A. Link. 2017. The first 50 years of the North American
Breeding Bird Survey. *Condor* 119:576–593.

710

Smith, A. C., M. A. R. Hudson, C. M. Downes, and C. M. Francis. 2015. Change points in the
712 population trends of aerial-insectivorous birds in North America: synchronized in time across
species and regions. *PLoS ONE* 10:e0130768.

714

Sørbye, S. H., and H. Rue. 2014. Scaling intrinsic Gaussian Markov random field priors in
716 spatial modelling. *Spatial Statistics* 8:39–51.

Soykan, C. U., J. R. Sauer, J. G. Schuetz, G. S. LeBaron, K. Dale, and G. M. Langham. 2016.
718 Population trends for North American winter birds based on hierarchical models. *Ecosphere*
720 7:e01351.

Thogmartin, W. E., J. R. Sauer, and M. G. Knutson. 2004. A hierarchical spatial model of avian
722 abundance with application to cerulean warblers. *Ecological Applications* 14:1766–1779.
724

Thogmartin, W.E., M.G. Knutson, and J.R. Sauer. 2006. Predicting regional abundance of rare
726 grassland birds with a hierarchical spatial count model. *Condor* 108:25-46.

Thomas, C. D., and J. J. Lennon. 1999. Birds extend their ranges northwards. *Nature* 399:213.

728

Waller, L. A., and C. A. Gotway. 2004. *Applied spatial statistics for public health data*. John
730 Wiley and Sons, New York, New York, USA.
732

Zhang, J., W.D. Kissling, and F. He. 2013. Local forest structure, climate and human disturbance
734 determine regional distribution of boreal bird species richness in Alberta, Canada. *Journal of*
Biogeography 40:1131-1142.
736

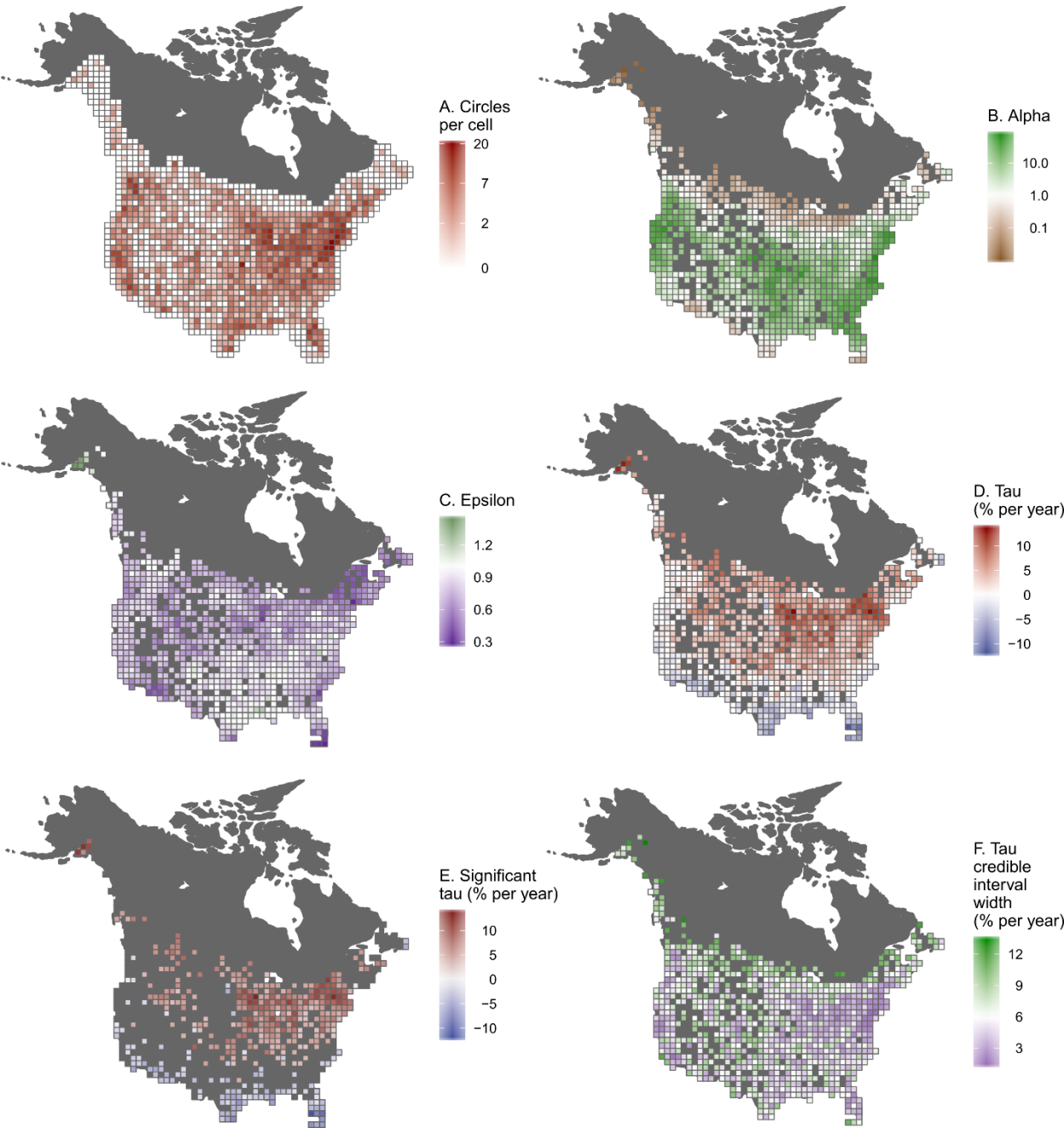
Zuckerberg, B., D. N. Bonter, W. M. Hochachka, W. D. Koenig, A. T. DeGaetano, and J. L.

738 Dickinson. 2011. Climatic constraints on wintering bird distributions are modified by
urbanization and weather: wintering birds, weather, food, and climate. *Journal of Animal*
740 *Ecology* 80:403–413.

742 **SUPPORTING INFORMATION**

All code and data needed to reproduce the SVC analysis is available at

744 <https://github.com/tmeeha/inlaSVCBC>.



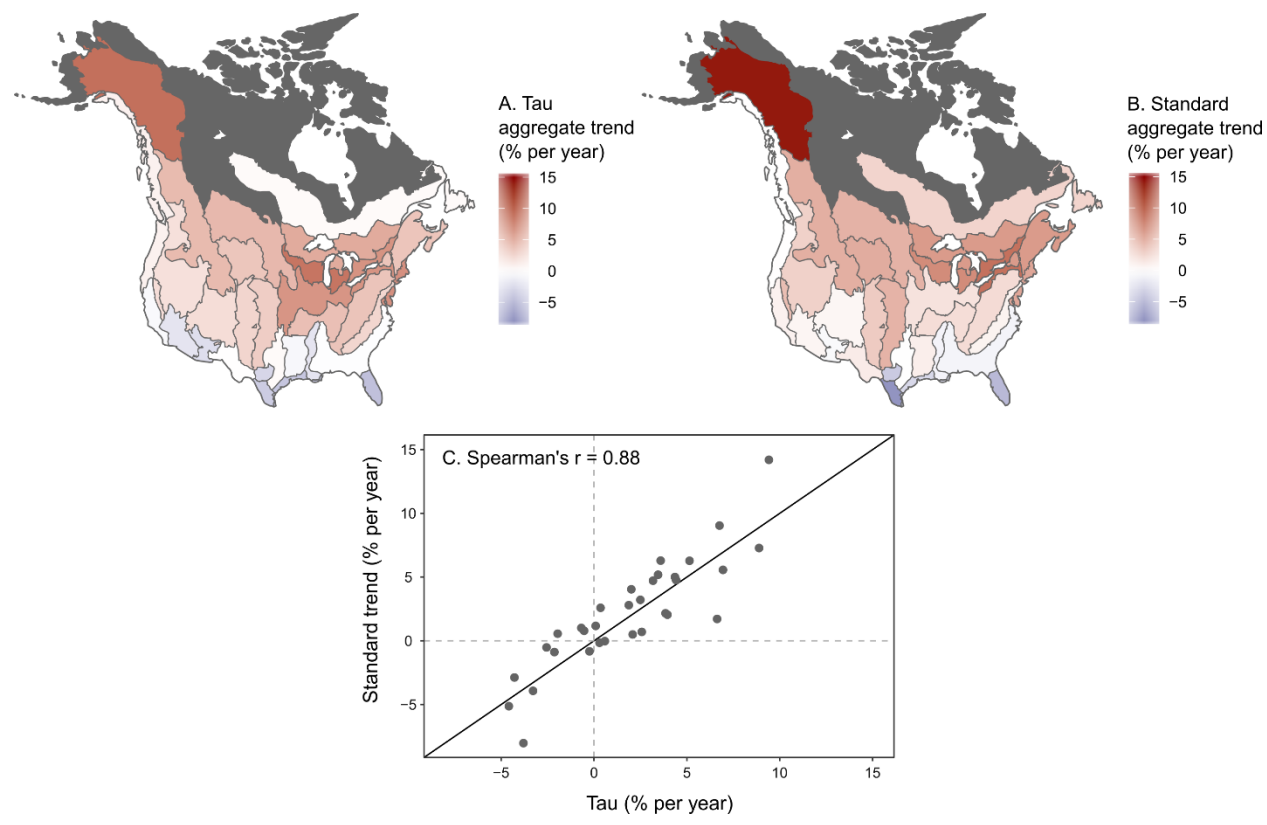
748

750

Fig. 1. Select inputs and outputs to the SVC model, including: (A) a map of the grid cell

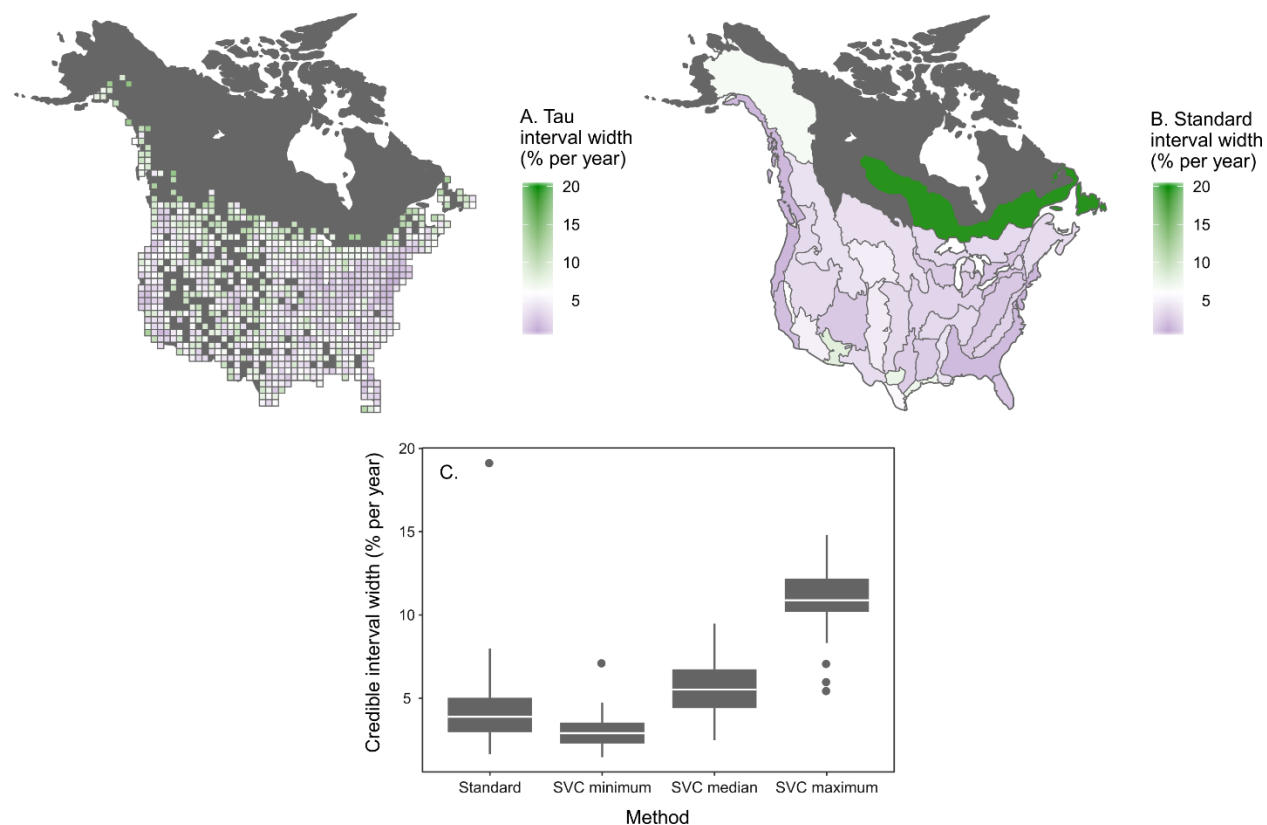
752 structure used in the American Robin analysis, along with the number of CBC circles included in
each cell; (B) α_i , representing the relative abundance index for 2017; (C) ϵ_i , representing the
754 effort-effect exponent; (D, E) τ_i , representing the long-term log-linear trend as percent change
per year per grid cell. Note that values shown in E are significantly different from 0, based on (E)
756 95% credible intervals for τ_i .

758 **Fig. 2**



760
762 Fig. 2. Comparison of posterior median trends for American Robin, aggregated to Bird
764 Conservation Regions, produced by (A) SVC and (B) standard methods, showing spatial
766 variation in their relationships and their pairwise correlation (C). The dark grey diagonal line in
768 C represents equality.

770 **Fig. 3.**

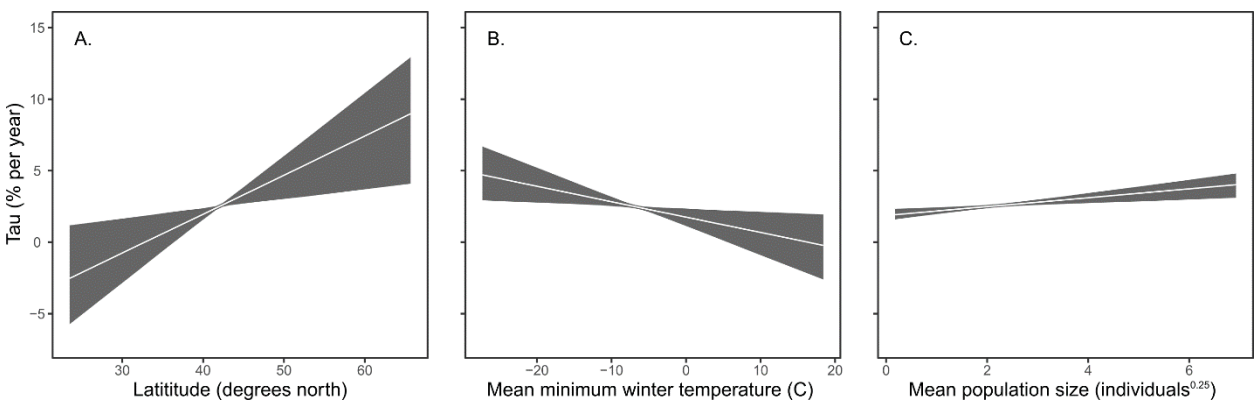


774 Fig. 3. Comparison of 95% credible interval widths for (A) estimates of τ_i (Tau, long-
term log-linear trend, percent change per year per grid cell) from the American Robin SVC
776 model and (B) analogous trends produced using the standard analysis and aggregated to Bird
Conservation Regions, shown as maps and (C) summarized with box plots.

778

780 **Fig. 4.**

782



784

786

Fig. 4. Model predictions and 95% credible intervals illustrating associations between American Robin SVC trends and (A) degrees north Latitude, (B) mean minimum winter

788

temperature between 1965 and 2017, and (C) mean human population size between 1971 and 2015.